Environ. Sci. Technol. **2006**, *40,* 2635−2643

Coupled Partitioning, Dilution, and Chemical Aging of Semivolatile Organics

N. M. DONAHUE,*,† A. L. ROBINSON,† C. O. STANIER,‡ AND S. N. PANDIS†

Center for Atmospheric Particle Studies, Carnegie Mellon University, Pittsburgh Pennsylvania 15213; Department of Chemical Engineering, University of Iowa, Iowa City, Iowa 52242

A unified framework of semi-volatile partitioning permits models to efficiently treat both semi-volatile primary emissions and secondary organic aerosol production (SOA), and then to treat the chemical evolution (aging) of the aggregate distribution of semi-volatile material. This framework also reveals critical deficiencies in current emissions and SOA formation measurements. The key feature of this treatment is a uniform basis set of saturation vapor pressures spanning the range of ambient organic saturation concentrations, from effectively nonvolatile material at 0.01 μg m^{-3} to vapor-phase effluents at 100 mg m^{-3}. Chemical evolution can be treated by a transformation matrix coupling the various basis vectors. Using this framework, we show that semi-volatile partitioning can be described in a self-consistent way, with realistic behavior with respect to temperature and varying organic aerosol loading. The time evolution strongly suggests that neglected oxidation of numerous "intermediate volatility" vapors (IVOCs, with saturation concentrations above ~1 mg m^{-3}) may contribute significantly to ambient SOA formation.

1. Introduction

Many authors have discussed the partitioning of semi-volatile organics (SVOCs) (*1*−*3*), and while it is certain that organics maintain coexistence among the phases present, the certainty ends there. Specifically, the identity of most SVOCs is unknown (*4, 5*), and it is impossible to build an accurate phase diagram for this variable mixture from first principles, much less to implement one efficiently in atmospheric models.

The key question is the partitioning, which we shall represent with a partitioning coefficient, ξ_i (the ratio of the concentration of compound *i* in the condensed phase. Its total concentration in the atmosphere). This may be determined by absorptive or adsorptive interactions over a complex (possibly externally mixed) background of particles. Those particles typically contain not only organics but elemental (black) carbon and inorganic ions such as sulfate, nitrate, ammonium, sodium, and chloride. While there is ample evidence that simple model systems (for example, mixed organic acids (*6*−*8*)) contain at least two organic phases, here we shall share with all air-quality models the assumption that partitioning over a single condensed phase satisfactorily represents the atmosphere. Testing this asumption is a first-order need.

There is no prospect of an exhaustive model of partitioning based on specific compounds; the aerosol comprises too many compounds, and far too few are identified. As a consequence, organic aerosol models must be based on aggregate characteristics. These treatments have evolved from division of material between "nonvolatile" and "volatile" fractions to parametrizations of semi-volatile compounds with bulk volatilities. Treatment of secondary organic aerosol (SOA), derived from in situ oxidation of volatile precursors, has evolved from positing a nonvolatile reaction product with a fixed (small) yield (*9*) to fits of chamber yield experiments, assuming one or two semi-volatile products where both the product yields and their volatilities are treated as free parameters (*10*). At present, primary emissions are treated as nonvolatile in models, remaining entirely in the condensed phase, though a recent analysis of dilution sampling data shows that they too should be treated using partitioning theory (*11*).

Almost all organic material associated with the condensed phase should be regarded as semi volatile. As a working definition, SVOCs include any compound with more than 1% of its mass in both the condensed and vapor phases somewhere in the atmosphere. Given the atmospheric range of organic aerosol (OA) mass concentrations of between 0.1 and 100 μg m^{-3} (*12, 13*), compounds with effective saturation concentrations between 0.001 and 10 000 μg m^{-3} should be considered semi-volatile under even the most narrow definition of the term.

However, there has been almost no effort to treat the subsequent chemical evolution of SVOCs in the atmosphere. The "products" in multiple-product models are aggregates representing from several to hundreds of compounds. Consequently, the prospects for treating chemistry explicitly are dim, threatening only a profusion of surrogate compounds with unique yields and volatilities. Chemistry will occur in both the vapor and condensed phases, and it will certainly alter volatilities. An especially important fraction consists of compounds with saturation concentrations just higher than the range described above. These "intermediate volatility" organic compounds (IVOCs) with saturation concentrations ranging from 1000 to 100 000 μg m^{-3} (1 to 100 mg m^{-3}) are found almost entirely in the vapor phase but have a very high potential to generate lower volatility products after reaction. They are not the traditional SOA precursors, which are typically much more volatile. For the sake of simplicity, "SVOC" in this paper will be taken to include both the SVOCs and IVOCs described above.

The goal of this paper is to create a unified framework for considering SVOCs. This framework provides a self-consistent description for semi-volatile partitioning of both SOA formation and primary emissions as well as the effects of temperature and chemistry on this partitioning. We project SVOCs onto a common basis set of saturation concentrations, and then develop coupling matrixes for both the gas and condensed phases to describe the evolution of volatility driven by temperature changes and chemistry. That chemistry includes oxidation in both phases as well as other condensed-phase processing, such as oligomerization. In this way, semi-volatile primary emissions, semi-volatile SOA, and chemical aging can be unified in a common treatment that is ideally suited to regional and global chemical modeling.

2. Basic Partitioning

We shall assume that absorptive partitioning dominates for SVOCs. This appears to be true for most cases in the atmosphere, unless the ratio of organic to elemental carbon

* Address correspondence to either author.
† Carnegie Mellon University.
‡ University of Iowa.

10.1021/es052297c CCC: $33.50
Published on Web 03/16/2006

(OC/EC) is especially low (*11*). If we consider a certain mass concentration of condensed-phase organic molecules, C_{OA}, we can define a partitioning coefficient ξ_i for some compound i, given a effective saturation concentration C_i.

$$\xi_i = \left(1 + \frac{C_i^*}{C_{OA}}\right)^{-1}; \; C_{OA} = \sum_i C_i \, \xi_i \qquad (1)$$

This shows the fraction of compound i found in the condensed phase, as well as the total organic aerosol concentration given a set of organic compound concentrations in all phases, C_i. Note that C_{OA} is the *total* mass concentration of organic aerosol, not just the carbon mass concentration. Some formulations (*2, 3, 16, 17*) use a partitioning coefficient K_i, which is the inverse of C_i^*. We prefer C_i^* and ξ_i because they describe the simple Hinshelwood saturation curve shown in eq 1; when $C_i^* \gg C_{OA}$, ξ_i will increase linearly with increasing organic mass, but eventually it will literally saturate, and the condensed-phase fraction will level off (at 1). A derivation of C^* is discussed in the Supporting Information, but in many ways, it is best regarded as an intrinsic, if empirical, property of aggregate condensed-phase compounds with similar volatilities.

As an example, if $C_{OA} = 1\ \mu g\ m^{-3}$ and a given compound has $C_i^* = 1\ \mu g\ m^{-3}$, we would expect 50% of the mass of that compound to be found in the condensed phase and 50% in the vapor phase. In this case, any compound with $(0.01 \leq C_i^* \leq 100)\ \mu g\ m^{-3}$ would have a significant mass fraction in both the vapor and condensed phases.

Equation 1 must be solved iteratively for C_{OA}, but the overall partitioning of any distribution of organic material can be recovered with good fidelity using a basis set of C^* values separated by factors of 10 (*17*). Because the atmosphere itself shows great variability, we use the following basis set:

$$\{C_i^*\} = \{0.01, 0.1, 1, 10, 100, 1000, 10\,000, 100\,000\}\ \mu g\ m^{-3} \qquad (2)$$

defined at 300 K. The least volatile fraction, at 10 ng m^{-3}, can describe the least volatile organics in the atmosphere, even in remote locations with $C_{OA} = 0.1\ \mu g\ m^{-3}$, only 10% of this material will be in the vapor phase. Under polluted conditions with $C_{OA} = 100\ \mu g\ m^{-3}$, about 0.1% of the 100 mg bin is in the condensed phase. However, one could add more bins at either end of the range to describe extreme conditions.

The consequences of eq 1 are easily summarized in a cartoon, shown in Figure 1a. In this figure, we see a plausible atmospheric distribution of compounds, cast onto the basis set specified in eq 2, and then partitioned according to eq 1. The total mass concentration, C_i, in each bin, C_i^*, is shown by a bar, with the filled (green) portion indicating the condensed-phase portion for each bin, $\xi_i\ C_i$. Only material with a saturation concentration within about 1 order of magnitude of the ultimate OA mass concentration ($C_{OA} = 10\ \mu g\ m^{-3}$ in this example) is significantly represented in each phase. Equation 1 is identical to an amplifier gain curve, and the reasonably linear range of this curve lies in the range $0.1 < \xi < 0.9$. This is why the proposed decadal spacing of the basis vectors is optimal. At the outside, basis vectors could be separated by a factor of 100 to retain some fidelity; such an efficient, low-resolution representation may be appropriate for global modeling.

The loadings for each bin in Figure 1a are an educated guess. We know that the mass emissions from primary sources, especially combustion sources, are characterized by a very broad array of compounds with a maximum flux for relatively volatile material (*11*, *18*, *19*). We also know that oxidation of individual SOA precursors often produces more relatively volatile material than relatively nonvolatile material (*16*, *20*–*22*). Filter-based measurement methods of SVOCs are especially prone to bias, but there is evidence that vapor-phase semi-volatiles exceed condensed-phase organics. For example, comparisons of bulk OC measurements using standard quartz and carbon-impregnated quartz filters during the Pittsburgh Air Quality Study (PAQS) (*23*) indicate that gas-phase semi-volatile organics exceed condensed-phase organics by a factor of 4 to 5, and in situ tandem-DMA measurements clearly show that ambient particles dominated by organic motor-vehicle emissions measured adjacent to a highway are relatively volatile upon heating (*24*).

The IVOCs will receive particular attention in this paper. In Figure 1a these are in the three right-hand bins. They do not represent a major fraction of the gas-phase reduced carbon; most major gas-phase organics, even commonly studied SOA precursors, have saturation concentrations well over 1 g m^{-3}. However, the IVOCs almost certainly contain more mass than the actual condensed-phase OA. For example, in Figure 1a, the fraction between 1 and 100 mg m^{-3} is completely vapor and holds, in total, 19.5 $\mu g\ m^{-3}$, compared to 10 $\mu g\ m^{-3}$ of OA. Because it fits into neither the particulate nor the gas-phase budget in any convenient way, this fraction is ignored in current models of local, regional, and global aerosol distributions. This may be a serious error.

3. Evolving Partitioning

The partitioning of compounds $\{C_i\}$ cast onto the basis set $\{C_i^*\}$ and described by eq 1 will evolve as an air parcel moves. This will happen for at least four reasons. First, fresh emissions will augment $\{C_i\}$ and, consequently, increase C_{OA}. The advantage of the basis-set formulation is that new sources may be added to a model without any additional cost, because the basis set specifies only saturation concentration and thus accommodates new compounds trivially. Second, the air mass may mix with another air mass, which will again change $\{C_i\}$ and alter C_{OA}. Third, temperature may change. This does not change $\{C_i\}$ at all, but instead the values of $\{C_i^*\}$ will shift with temperature, some material will repartition, and C_{OA} will change. Finally, chemical reactions will transform the distribution, moving mass from one bin to another. If sufficient material is moved from high-volatility bins to low-volatility bins, the consequence will be an increase in C_{OA} analogous to SOA production from known precursors.

3.1. Dilution. Semi-volatile emissions enter the atmosphere and rapidly mix with background air. This mixing cools and dilutes the emissions, which significantly changes the gas-particle partitioning. Cooling will be discussed below, but here we shall address dilution, both by clean air and background air also containing SVOCs. Vehicular emissions are eventually diluted by a factor of 1000 or more (*11*), but dilution near roadways is much lower (*25*). Recent findings relating health consequences to distances from major roadways underscore the importance of accurately describing particle behavior as the dilution ratio evolves in the atmosphere (*26*).

Dilution sampling was developed to simulate these processes in a controlled way (*27*). This approach has been used to characterize emissions from a variety of sources, including vehicular emissions (*19, 28*), coal combustion (*29*), biomass burning (*30*), and cooking (*31*). Very recently, dilution sampling results for organic-rich sources have been cast in the framework of the partitioning theory underpinning the present work, using a conventional two-product model and revealing that both wood-smoke and exhaust show significant semi-volatile behavior (*11*).

Figure 1b shows a plausible distribution of emissions from a primary organic aerosol source such as a gasoline or diesel engine. This assumed distribution is consistent with measurements of the organic composition of diesel (*18*) and

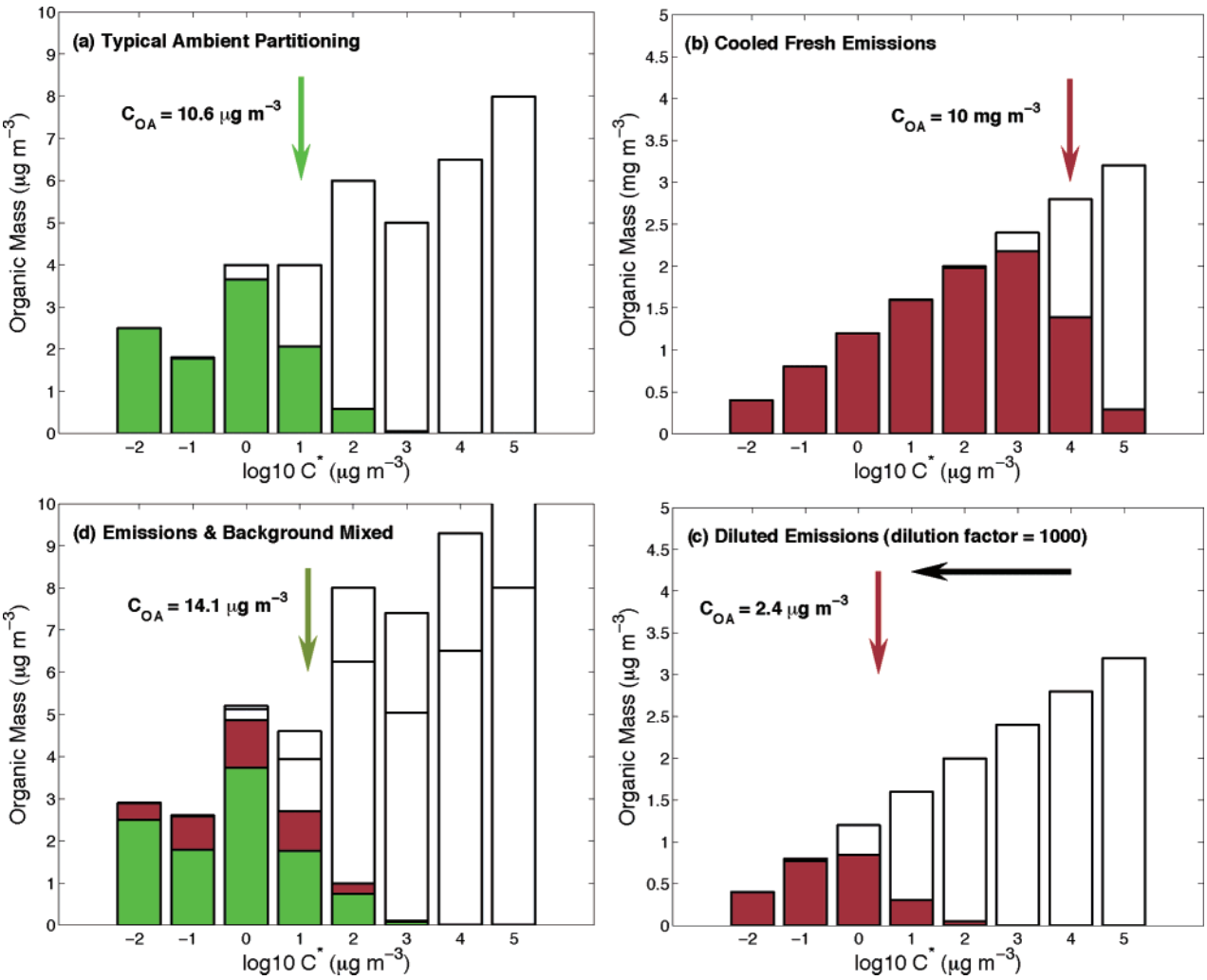

FIGURE 1. (a) Partitioning of a collection of semi-volatile compounds, with total loadings (in μg m^{-3}) shown with full bars and the condensed-phase portion with filled (green) bars. Compounds are distributed according to their mass-equivalent effective saturation concentration (C^*, also in μg m^{-3}), which is presented as a logarithmically distributed basis set. $C_{OA} = 10.6$ μg m^{-3}, shown with an arrow, and so that bin is evenly split between the two phases. (b) Semi-volatile emissions as they might appear near the output of a primary source, before substantial dilution into the background atmosphere (only enough dilution to cool the emissions to ambient temperature is assumed). The high loading leads to partitioning well into the high C^* end of the distribution, as shown in brown. Note the scale of the *y* axis (mg m^{-3}), which is a factor of 1000 greater than the scale on the other figures. (c) The effect of dilution by pure air on the emissions depicted above. The dilution factor of 1000 is indicated with a horizontal black arrow. Dilution by a factor of 1000 reduces the aerosol mass by a factor of 4000 because of repartitioning into the vapor phase. (d) The effect of dilution, as depicted in panel b above but now into background air represented in panel a above. The partitioning of the background organic material and the fresh emissions are kept separate, in green and brown, only for illustrative purposes. The vapor portions of the background and the fresh emissions are also separated, though each is shown with a white bar. Note that both the background and fresh emissions are partitioned more toward the condensed phase than in panels a or d, instead of 12.4 μg m^{-3} there are 14.1 μg m^{-3} and the condensed-phase mass due to the fresh emissions is almost doubled.

gasoline (*19*) engine exhaust. We must use an assumed distribution in the example because less than half of organic mass of the emissions have been characterized on a compound-by-compound basis. However, unspecific, carbon-number-based chromatography has achieved good mass recovery (*4*). These observations are consistent with the distributions shown here, and they are also consistent with dilution-sampling data from primary emission sources (*11*). The concentrations $\{C_i\}$ in Figure 1b are very high (the *y* axis is in mg m^{-3}) because we assume we are near the exhaust, with only enough dilution to achieve ambient temperature. Figure 1b also shows the partitioning of the emissions, which result in $C_{OA} = 10$ mg m^{-3}. This is a factor of 1000 greater than the ambient case shown in Figure 1a, but it is representative of the highly concentrated conditions occurring near the emission point of a heavily emitting source.

It is standard practice to discuss dilution sampling in terms of the *dilution ratio* of the experiment. While this is an important parameter, it would be far more revealing to represent results in terms of the ultimate particulate organic mass C_{OA} achieved; it is this, and not the dilution ratio, that determines the ultimate partitioning described by eq 1. Also, it is important that dilution experiments reach low C_{OA} levels (1 μg m^{-3} or less) to accurately assess partitioning under ambient conditions. The resulting partioning of the mixture depicted in Figure 1b diluted by a factor of 1000 to reach ambient levels is shown in Figure 1c (the *y* axis is now in μg m^{-3}). With this dilution, C_{OA} drops by a factor of 4000 due to repartitioning.

The change in OA with dilution represented by Figures 1b,c is exactly the behavior observed when measuring both engine and wood combustion emissions with dilution

samplers. This behavior has been reproduced using a more conventional two-product partitioning model, with a "more volatile" fraction ($C^* \simeq 1500\ \mu g\ m^{-3}$) and a "less volatile" fraction ($C^* \simeq 25\ \mu g\ m^{-3}$) (*11*). Here, we have mapped these two components onto the basis set $\{C_i^*\}$, using both the results of the two-component model (*11*) and the speciated emissions data (*18, 19*) as a guide.

The case illustrated in Figure 1c depicts dilution with air completely devoid of either particulate matter or vapor-phase organics; this is how dilution samplers are typically operated. In the atmosphere, of course, emissions are diluted with ambient air that does contain SVOCs. The effect of this background pollution on the partitioning can be illustrated by combining the fresh emissions shown in Figure 1b with the typical ambient conditions shown in Figure 1a, in appropriate proportions. If the same dilution scenario depicted in Figure 1c is carried out with dilution air characterized by Figure 1a, the result is the distribution of SVOCs shown in Figure 1d. Because of the SVOCs in the background air, less of the emissions will vaporize than in the clean-air case; in fact, some of the SVOCs in the background air will condense, due to the increased C_{OA}. The net effect is that mixing of $10\ \mu g\ m^{-3}$ background air with the fresh emissions yields $14.1\ \mu g\ m^{-3}$ of total particulate organic carbon, and increase of $4.1\ \mu g\ m^{-3}$, even though the same degree of dilution with clean air yields only $2.4\ \mu g\ m^{-3}$. The extra $1.7\ \mu g\ m^{-3}$ comes from repartitioning of vapors from both the background air and the emissions back into the condensed phase.

In Figure 1d we separate the background condensed phase (green) from the primary emissions condensed phase (brown) to illustrate each contribution (the two different vapor phase contributions are also shown with open bars, emissions above background). This is a simple example of how one can carry out source attribution with parallel bins, one for a specific source and one for the background; however, it also reveals a challenge as the "blame" for the extra $1.7\ \mu g\ m^{-3}$ is difficult to assign.

Current models represent primary organic emissions as non volatile. This is clearly incorrect for at least three reasons: the partitioning near the source will be neglected; evaporation while emissions are diluted with progressively cleaner background air will be neglected; and the role of the IVOCs will be completely missed. Consequently, both near-source issues such as roadway exposure hazards and regional to global issues, such as oxidation, will be misrepresented. Furthermore, there is additional clear evidence that the condensed-phase organics in vehicular emissions are volatile: when these particles are heated, they shrink (*11, 24*).

3.2. Temperature Dependence. As compounds are warmed, they tend to vaporize. For a basis set of saturation concentrations $\{C_i^*\}$ such as we are considering here, the effect of increasing temperature will be to shift the basis set toward higher *C*s*. As temperature rises some material (with a certain C^* near C_{OA}) will "cross the volatility threshold" and vaporize. This is important to model correctly, both to treat hot primary emissions sources and to properly reproduce the effect of changing ambient temperature; an analogy is nitrate, which is far less volatile in winter than in summer, and thus tends to partition more to the condensed phase in winter.

The important parameter for the temperature dependence of *C*s* is the enthalpy of vaporization ΔH_v. Measurements and estimates for specific low-volatility compounds give enthalpies of vaporization between 40 and 110 kJ mole^{-1} (*32, 33*), with the higher values corresponding to lower-volatility species. Data tend to be confined to compounds with *C*s* of well over $10\ \mu g\ m^{-3}$ because the experiments are very difficult at lower volatility. On the other hand measurements of the temperature dependence of aggregate organic aerosol suggest an overall temperature dependence equivalent to 40 kJ mole^{-1} or less, even for organic aerosol loadings of $10\ \mu g\ m^{-3}$ and less (*22*), where theory predicts values over 100 kJ mole^{-1} (*30*). Consequently, two-component partitioning models need to include unphysically low enthalpies of vaporization in order to reproduce the observed shallow temperature dependence of both primary and secondary organic aerosol (*11, 34*).

An important note on terminology is that it is wrong to conflate "volatile" with "strong temperature dependence". Low saturation concentration (low volatility) compounds will generally have very high enthalpies of vaporization (*33*), and so under the proper circumstances, they will show a much stronger temperature dependence than higher saturation concentration compounds. The proper circumstances are *C*s* near enough to the condensed-phase concentration for a change in temperature to significantly change the condensed-phase mass.

With a roughly constant entropy of vaporization, the factor of 10 spacing in saturation concentration, described by eq 2, corresponds to a succession of enthalpies (ΔH_{vap}) separated by 700 K, or 5.8 kJ/mol. The question is whether we can reproduce the observed shallow temperature dependence using a distribution of products with different *C*s* and the expected values for ΔH_v.

We shall consider a test case with SVOCs distributed over a range of *C*s* from $C^* = 1$ ng m^{-3} to 100 mg m^{-3} at 300 K, with somewhat more material in the higher C^* bins. This is, again, consistent with both primary emissions (*18, 19*) and SOA formation (*35*). We shall assume an ΔH_v for the $1\ \mu g\ m^{-3}$ material of $12\ 000\ K \simeq 100$ kJ mole^{-1}, which increases by 700 K for each lower C^* bin and decreases by 700 K for each higher C^* bin (i.e. $\theta_v = 12\ 000\ K - \log_{10}(C^*/(1\ \mu g\ m^{-3})) \times 700\ K$). Changing the temperature shifts the basis set left and right; the bins converge slightly with increasing temperature under these assumptions but never overlap because the lower C* bins have larger values of ΔH_v, but all have the same S_v

We can then easily calculate the partitioning over a range of temperatures, for this example we will use 285−310 *K*, which roughly equals the temperature range of 15−40 C reached in the Carnegie Mellon smog chamber (*22*). We shall consider a low-mass and a high-mass case, with the low-mass case yielding $C_{OA} \simeq 2.8\ \mu g\ m^{-3}$ at 300 K and the high-mass case (with 50 times the total organic concentration) yielding $C_{OA} \simeq 268\ \mu g\ m^{-3}$ at 300 K.

The basic temperature effect is shown in Figure 2, which shows the aerosol partitioning for 310 K ($C_{OA} = 2.1\ \mu g\ m^{-3}$ on top) and 285 K ($C_{OA} = 4.0\ \mu g\ m^{-3}$ on bottom). The *C*s* shift to the right with increasing temperature, causing the total aerosol mass to drop by a factor of 2 between 285 and 310 K. This is quantitatively consistent with the aerosol volume changes seen in numerous SOA experiments in our laboratory (*22, 35*).

Overall, the effect of temperature on the aerosol partitioning for both high and low total loading is shown in Figure 3, with the low loading ($2.8\ \mu g\ m^{-3}$ at 300K) case shown in blue squares and the high loading ($268\ \mu g\ m^{-3}$) case shown in green circles. The figure shows the normalized mass, using 290 K as the reference. This follows the treatment in Stanier et al. (*22*), with very similar results; while there is a difference between the two curves, with slightly less mass change at higher loading, this difference is within the noise of the experimental data. Furthermore, the data cover a narrower range of total mass than this test case, and the actual distribution of mass over the vapor-pressure basis set assumed here is not directly constrained by any data, it is a phenomenological guess.

The modeled aerosol mass roughly doubles with a 25 °C drop in temperature. If this were analyzed for an effective single-component ΔH_v, the result would be of order 40 kJ

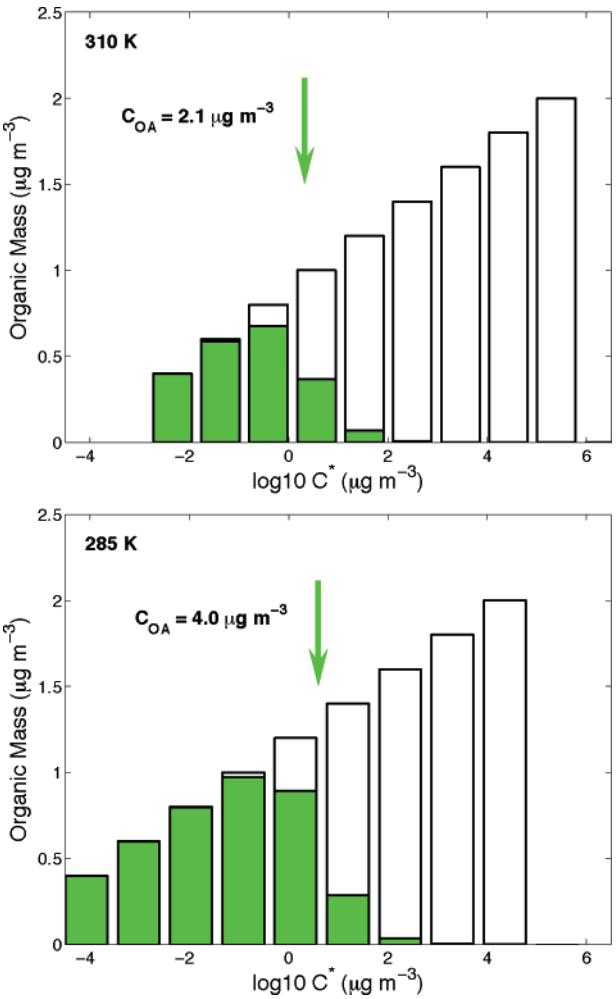

FIGURE 2. Temperature dependence. A basis set of saturation concentrations (ranging from 1 ng to 100 mg at 300 K) changes with temperature according to the Clausius Clapeyron equation. The enthalpy of vaporization for the 1 μg (at 300 K) fraction is assumed to be 100 kJ/mol. Less volatile fractions have higher vaporization enthalpies, while more volatile fractions have lower values (see text). Heating (upper panel) shifts the basis set to the right, while cooling shifts to the left. As a consequence, the total condensed-phase mass changes by roughly a factor of 2 over 25 K, consistent with observations.

mole^{-1}. The low effective temperature dependence is caused by the relatively small aerosol mass crossing the volatility threshold (the green arrow in Figure 2) as the temperature increases. It is a direct consequence of the distribution of *C*s*. Our conclusion is that the chamber data are consistent with the magnitude and range of enthalpies expected of these semi-volatile compounds. The bottom line is that models should not confuse two possible approaches; models with few semi-volatile components should use artificially low enthalpies of vaporization, while models with numerous components covering a wide range of *C*s* should use the more realistic enthalpies of vaporization considered here. The realistic option is vastly preferable, as the former option will behave badly as additional components are added to the model, either through primary emissions or secondary chemistry.

3.3. Chemistry. If one reason for tracking the full range of *C*s* for organics is direct condensed-phase partitioning, a far more pressing reason is chemistry. These SVOCs are, at most, partially oxidized, and they will undergo oxidation in all phases. From the perspective of our basis set, the consequence of this oxidation will be to move material from

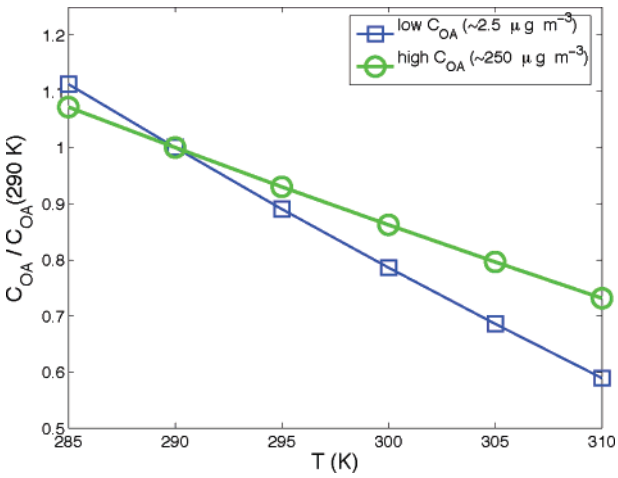

FIGURE 3. Normalized change in aerosol volume (or mass) for two different loadings: a low loading shown in blue and seen in Figure 2 and a much higher loading (with 50 times more material) shown in green. Both show roughly the same temperature dependence, the exact behavior of real material will depend on the distribution of material over the saturation concentration basis set but should not differ too far from a rough 1−2% per K.

one bin to another. By redistributing material, the chemistry will, without a doubt, alter the partitioning, and thus C_{OA}. The question is, how important this will be and how to model it.

Secondary chemistry in the condensed phase may increase the aerosol concentration, possibly through oligomerization (*36*−*38*), or decrease the aerosol concentration (*39, 40*) by cleaving off low carbon-number oxidized organic compounds. The essential facts are that many volatile compounds, when oxidized, yield a substantial fraction of less volatile products (this drives SOA formation), but that the end product of oxidation would be CO_2 if the system were allowed to evolve to equilibrium. Many second-generation oxidation products will be less volatile than their first-generation precursors. Consequently, there must be an "aerosol generation number" where the aerosol yield is at a maximum (*41*).

Oxidants including OH, ozone, and NO_3 may initiate this oxidation. We expect OH radical to be the dominant oxidant, but ozone will play a role, oxidizing unsaturated compounds in the gas phase as well as, possibly, others in the condensed phase. Likewise, photolysis will grow progressively more likely as the compounds become more oxidized. Simple comparison with other organics suggests that the gas-phase lifetimes of the vapors will be of order 1 day (*41*). The condensed-phase lifetime remains quite uncertain, but again, simple scaling of radical uptake studies (*39*), as well as evidence from tracer measurements, suggests that lifetimes are not more than a few days (*42*).

Conventional SOA experiments (*9, 21, 22*) focus on precursors with high mass emissions but also very high *C*s*. These include the monoterpenes, trimethyl benzene, the xylenes, and such. Most precursors in the SOA literature have vapor pressures within an order of magnitude of 1 mb, which corresponds $C^* \simeq 1$ g m^{-3}, or more than a factor of 1000 higher than the highest C^* in the basis set we are considering here.

This basis-set representation enhances the design and interpretation of conventional chamber SOA experiments. First, it emphasizes the need to extend experiments to ambient C_{OA} levels, as we have recently shown (*43*), because the basis vectors are only constrained by data with $C_{OA} = C^*$. Conventional "two-product" models contain four unconstrained degrees of freedom for each SOA precursor in a

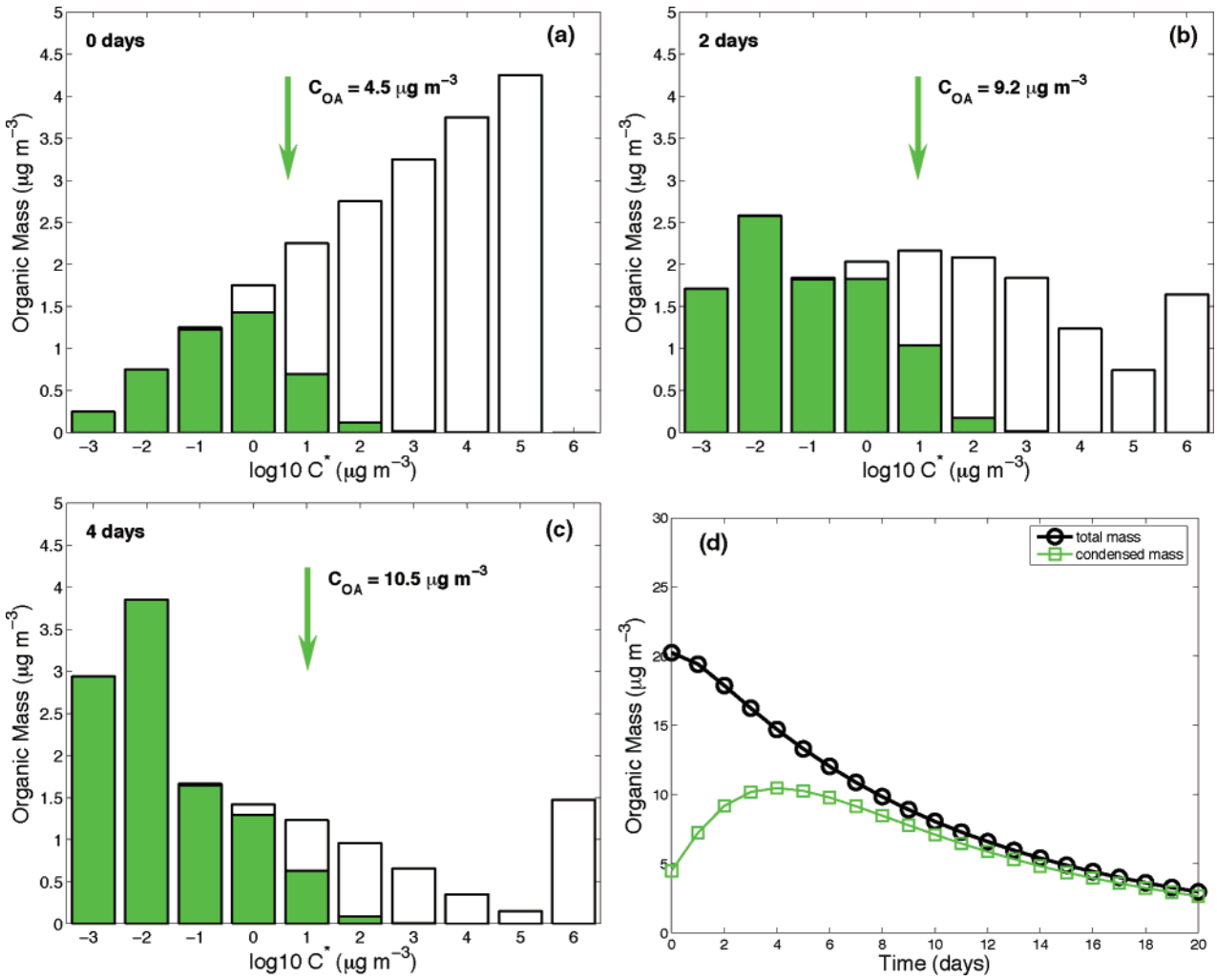

FIGURE 4. (a−c) Evolving mass distribution as semi-volatile organics are chemically processed to produce less volatile products (0 days, 2 days, and 4 days, see text). Chemistry eventually drives material into the high volatility bin (6) and then out of the model. (d). Time evolution of the total organic carbon (circles) and condensed-phase organic carbon (squares) in the simple model. With the particular assumed balance between formation of less volatile products and eventual formation of highly volatile products the aerosol mass roughly doubles after 4 days (4 generations), and then declines as the organics are oxidized more completely.

system. The basis-set representation contains one degree of freedom for each basis component included, and multiple components outside the range of data will cause singularities in fitting. No partitioning model can accurately extrapolate, because we have no a priori knowledge of volatility distributions in these complex systems. For example, if data for α-pinene + ozone SOA extend to 10 μg m^{-3}, and we have a basis set with low-volatility components at {0.1, 1, 10} μg m^{-3}, the data can be fit with equal fidelity with constrained low-volatility yields {α_1, 0, 0} or {0, 0, α_3}. However, extrapolations to C_{OA} < 10 μg m^{-3} will diverge dramatically.

It appears that relatively few compounds dominate biogenic emissions, with mono- and sesquiterpenes receiving the bulk of the attention for SOA formation. In addition, isoprene so dominates biogenic VOC mass emissions that even a small SOA yield could greatly influence global SOA formation (*44, 45*). The reverse may also be true, however, with very high aerosol yields coming from a multitude of less volatile compounds totaling less than 10% of the total VOC mass flux. Anthropogenic emissions typically include thousands of compounds spanning the full range of *C*s* considered here (*18, 19*). Also, in many cases, the first-stage oxidation products of many volatile precursors appear to be relatively volatile, with more product mass with *C*s* above the 100 μg m^{-3} range than below it (*10, 20, 35*). Thus, while it is appropriate to consider the specific chemistry of the volatile, high-flux compounds, we also badly need a framework to consider the oxidation of the enormous collection of other compounds, including the first-generation oxidation products of those specific precursors.

We propose that models and experiments alike adopt the basis set of *C*s* presented here. Emissions and SOA formation from specific precursors can be cast onto the basis set, as we have shown. Furthermore, after this initial distribution, it is vitally important that chemistry continue in the model. Experiments should identify the "prompt" yields or emissions of semi-volatiles (distributed on the *C** basis set). This should not be confused with the evolving yields and evolving volatility driving by chemistry through aging, some oligomerization, or other phenomena. Of course, experimental elucidation of these phenomena is vital as well, and some are being reported (*5, 36*).

As shown in the Supporting Information, this chemistry can be represented by a transformation matrix that redistributes organic material among the various basis vectors. This can include gas- and condensed-phase chemistry, radical oxidation, and acid-catalyzed oligomerization. It will include reactions that decrease volatility of some material, but it must include loss that ultimately transforms material into highly oxidized volatile compounds.

3.3.1. A First-Order Example. We have very few experimental constraints on the oxidation of these SVOCs. As a simple test, we shall consider a case in which neither the chemical time scale nor the reaction products depend on which phase the oxidation occurs in. We shall assume that the oxidation in either phase is driven primarily by OH radicals with a time scale of roughly 1 day. This is consistent with gas-phase rate constants for large alkanes, which are typically 1×10^{-11} cm^3 sec^{-1} (*46*), given 10^6 cm^{-3} OH. It is reasonable for condensed-phase oxidation by OH as well (*42*).

A simple matrix equation describes the evolution of organic mass, $\vec{C}$, projected onto our C^* basis set:

$$\frac{d\vec{C}}{dt} = k\,(\boldsymbol{A}\text{-}\boldsymbol{I})\vec{C} \qquad (3)$$

where k is a characteristic first-order decay rate constant and $\boldsymbol{A}$ is a branching matrix. This matrix describes the saturation concentration of the oxidation products; it is also described in detail in the Supporting Information. In this simple example we shall assume that oxidation moves material, on average, to a slightly lower C^* (to the left on the axis), by one or 2 orders of magnitude per event. This is a much smaller shift than we often see in SOA yield experiments. However, every step also makes a small fraction very volatile material that will not partition to the condensed phase.(*40*)

The predictions of this model are shown in Figure 4. Figure 4a shows the initial distribution of the material across the saturation concentration basis set; this initial distribution is consistent with the examples shown in Figure 1. Figure 4b,c show the evolved distribution after 2 and 4 days, respectively. The total organic aerosol and total organic mass in both phases are shown in Figure 4d as a function of time. The organic aerosol mass more or less doubles in 4 days. The total mass decays away in 10 days because the assumed branching ratio into volatile products is 0.1 in our transformation matrix. The condensed-phase distribution rapidly becomes quite non volatile, and it also reaches a steady state (as a distribution) in about 4 days. With most of the condensed-phase material well below the volatility threshold, the temperature dependence of this aerosol will be weaker than that shown in Figure 3. By extension, aged organic aerosol is likely to show little temperature dependence in the atmosphere.

Obviously, many other phenomena will be in play in the real world, including deposition, dilution, and emission of fresh material. However, this exercise isolates the role of chemistry in the problem. There are a few estimates of the mean age or organic aerosol in the eastern U.S. based on ambient data, including results showing that the OA in Pittsburgh contains a very large regional compenent (*47*) and also an analysis of combined data from NEAQS indicating a peak in OA loading after approximately 48 hours (*48*). This later work shows a largely anthropogenic secondary contribution to OA in New England, consistent with our assumptions. The 48-time scale is the integral including the other phenomena neglected in our simple deposition and dilution-free box model. While the two results appear to be generally consistent, it remains to be seen whether inverse models of ambient data will be able to significantly constrain the **K** matrix or whether the laboratory results alone will do so.

4. General Discussion

The C^* basis set presented here is not the only set of properties likely to be required for accurate organic aerosol modeling; the basis set specifically targets semi-volatile partitioning and thus the total C_{OA}. Other basis directions could describe other important properties, such as hygrocsopicity, single scattering albedo, etc. (*49*) It may be that two dimensions, saturation vapor pressure and oxidation state, could adequately map the full range of organic aerosol properties. It may well be that more dimensions are required. This is a separate issue under consideration elsewhere [McFiggans, personal communication].

Several other basis directions come to mind quickly. For one, a simple oxidation-state basis containing two components could easily be added to the description, with a "hydrocarbon-like" endpoint perhaps corresponding closely to the observational HOA described in aerosol mass spectrometer (AMS) measurements (*50*) and an "oxidized" endpoint corresponding to the AMS OOA. The oxidized endpoint would have an oxygen-to-carbon ratio of roughly 1:1, and the hydrocarbon-like endpoint would have a 0:1 ratio. Each oxidation event would move a fraction of the material in a given saturation vapor pressure bin from the reduced to the oxidized state, no matter what happened to the C^*. Activity coefficients could well evolve with this transformation as well.

The key assumption for this work is that organics can be grouped by saturation concentration, and that, at least to first order, their subsequent development can be followed without regard to their specific identity. Regardless of the need to retain composition information, it is clearly important for SOA formation experiments as well as source dilution experiments to identify the full range of volatilities present in a given source or system; it is the distribution of these compounds, and not the specific aerosol yield or source strength in some experiments, that should be delivered to the aerosol partitioning module of a transport and chemistry model.

Both SOA yield experiments and source dilution experiments must cover the range of aerosol mass likely to be found in the atmosphere, something like $0.1 \rightarrow 50$ μg m^{-3}, to be fully useful for atmospheric modeling. Furthermore, there is a critical unknown: the behavior of the IVOCs through multiple generations of atmospheric oxidation. It is entirely possible that such material dominates the regional and global organic aerosol budget. Developing experiments that can constrain the behavior of this material in a way that even qualitatively resembles its atmospheric behavior is a serious challenge.

Supporting Information Available

Details about the partitioning theory, kinetic transformation, forms of chemistry likely to affect the organic aerosol mass. This material is available free of charge via the Internet at http://pubs.acs.org.

Acknowledgments

Although the research described in this manuscript has been funded wholly or in part by the United States Environmental Protection Agency through grants RD-83108101 and R832162, it has not been subjected to the Agency's required peer and policy review and therefore does not necessarily reflect the views of the Agency and no official endorsement should be inferred.

Literature Cited

(1) Pankow, J. An absorption model of gas/particle partitioning of organic compounds in the atmosphere. *Atmos. Environ.* **1994**, *28,* 185.
(2) Pankow, J. An absorption model of the gas/aerosol partitioning involved in the formation of secondary organic aerosol. *Atmos. Environ.* **1994**, *28,* 189.
(3) Pankow, J.; Seinfeld, J.; Asher, W.; Erdakos, G. Modeling the formation of secondary organic aerosol. 1. application of theoretical principles to measurements obtained in the

α-pinene/, β-pinene/, sabinene/, δ^3-carene/, and cyclohexene/ ozone systems. *Environ. Sci. Technol.* **2001**, *35,* 1164.
(4) Hildemann, L. M.; Mazurek, M. A.; Cass, G. R. Quantitative characterization of urban sources of organic aerosol by high-resolution gas chromatography. *Environ. Sci. Technol.* **1991**, *25,* 1311−1325.
(5) Baltensperger, U. et al. Secondary organic aerosols from anthropogenic and biogenic precursors. *Faraday Discussions* **2005**, *130,* 130/14.
(6) Parsons, M. T.; Knopf, D. A.; Bertram, A. K. Deliquescence and crystallization of ammonium sulfate particles internally mixed with water-soluable organic compounds. *J. Phys. Chem. A* **2004,** *108,* 11600-11608.
(7) Knopf, D. A.; Anthony, L. M.; Bertram, A. K.; Reactive uptake of O_3 by multiphase mixtures containing oleic acid. *J. Phys. Chem. A* **2005,** *109,* 5579−5589.
(8) Katrib, Y.; Biskos, G.; Buseck, P. R.; Davidovts, P.; Jayne, J. T.; Mochida, M.; Wise, M. E.; Worsnop, D. R.; Martin, S. T. Ozonolysis of mixed oleic-acid/steric-acid particles: Reaction kinetics and chemical morphology. *J. Phys. Chem. A* **2005,** *109,* 10910−10919.
(9) Pandis, S.; Paulson, S.; Seinfeld, J.; Flagan, R. Aerosol formation in the photooxidation of isoprene and β-pinene. *Atmos. Environ.* **1991**, *26,* 997.
(10) Odum, J.; Hoffmann, T.; Bowman, F.; Collins, D.; Flagan, R.; Seinfeld, J. Gas/particle partitioning and secondary organic aerosol yields. *Environ. Sci. Technol.* **1996**, *30*, 2580.
(11) Shrivastava, M.; Lipsky, E. M.; Staier, C. O.; Robinson, A. L. Modeling semi-volatile organic aerosol mass emissions from combustion systems. *Environ. Sci. Technol.* **2005**, *Submitted,*.
(12) Chung, S. H.; Seinfeld, J. H. Global distribution and climate forcing of carbonaceous aerosols. *J. Geophys. Res.* **2002**, *107,* 4407.
(13) Cabada, J. C.; Rees, S.; Takahama, S.; Khlystov, A.; Pandis, S. N.; Davidson, C. I.; Robinson, A. L. Mass size distributions and size resolved chemical composition of fine particulate matter at the Pittsburgh supersite. *Atmos. Environ.* **2004**, *38,* 3127−3141.
(14) Griffin, R.; Dabdub, D.; Seinfeld, J. Secondary organic aerosol 1, atmospheric chemical mechanism for production of molecular consituents. *J. Geophys. Res.* **2002,** *107,* 10.1028/2001JD00541.
(15) Utembe, S. R.; Jenkin, M. E.; Derwent, R. G.; Lewis, A. C.; Hopkins, J. R.; Hamilton, J. F. Modelling the ambient distribution of organic compounds during the August 2003 ozone episode in the southern UK. *Faraday Discuss.* **2005,** *130,* 311−326
(16) Kamens, R.; Jang, M.; Chien, C.; Leach, K. Aerosol formation from the reaction of α-pinene and ozone using a gas-phase kinetics-aerosol partitioning model. *Environ. Sci. Technol.* **1999**, 1430.
(17) Bian, F.; Bowman, F. M. Theoretical method for lumping multicomponent secondary organic aerosol mixtures. *Env. Sci. Technol.* **2002,** *36,* 2491.
(18) Schauer, J. J.; Kleeman, M. J.; Cass, G. R.; Simoneit, B. R. T. Measurement of emissions from air pollution sources. 2. C_1 through C_{30} organic compounds from medium duty diesel trucks. *Environ. Sci. Technol.* **1999**, *33,* 1578−1587.
(19) Schauer, J. J.; Kleeman, M. J.; Cass, G. R.; Simoneit, B. R. T. Measurement of emissions from air pollution sources. 5. C_1 through C_{32} organic compounds from gasoline powered motor vehicles. *Environ. Sci. Technol.* **2002**, *36,* 1169−1180.
(20) Odum, J.; Jungkamp, T.; Griffin, R.; Forstner, H.; Flagan, R.; Seinfeld, J. Aromatics, reformulated gasoline, and atmospheric organic aerosol formation. *Environ. Sci. Technol.* **1997**, *31*, 1890.
(21) Griffin, R.; Cocker, D.; Flagan, R.; Seinfeld, J. Organic aerosol formation from the oxidation of biogenic hydrocarbons. *J. Geophys. Res.* **1999**, *104,* 3555.
(22) Stanier, C. O.; Pandis, S. N. Measurements of the volatility of aerosols from α-pinene ozonolysis, *Environ. Sci. Technol.* **2006**, submitted.
(23) Subramanian, R.; Khlystov, A. Y.; Cabada, J. C.; Robinson, A. L. Positive and negative artifacts in particulate organic carbon measurements with denuded and undenuded sampler configurations. *Aerosol Sci. Technol.* **2004**, *38,* 27−48.
(24) Kuhn, T.; Biswas, S.; Fine, P. M.; Geller, M.; Sioutas, C. Physical and chemical characteristics and volatility of pm in the proximity of a light-duty vehicle freeway. *Aerosol Sci. Technol.* **2005**, *39,* 347−357 DOI: 10.1080/027868290930024.
(25) Zhang, K. M.; Wexler, A. S. Evolution of particle number distribution near roadways—part I: analysis of aerosol dynamics and its implications for engine emission measurement. *Atm. Environ.* **2004**, *38,* 6643−6653.
(26) Zhu, Y.; Hinds, W.; Kim, S.; Sioutas, C. Concentration and size distribution of ultrafine particles near a major highway. *J. Air Waste Manage. Assoc.* **2002**, *52,* 1032−1042.
(27) Hildemann, L.; Cass, G.; Markowski, G. A dilution stack sampler for collection of organic aerosol emissions- design, characterization and field-tests. *Aerosol Sci. Technol.* **1989**, *10,* 193−204.
(28) Rogge, W. F.; Hildemann, L. M.; Mazurek, M. A.; Cass, G. R. Sources of fine organic aerosol. 2. noncatalyst and catalyst-equipped automobiles and heavy-duty diesel trucks. *Environ. Sci. Technol.* **1993**, *27*, 636−651.
(29) Lipsky, E. M.; Robinson, A. L. Design and evaluation of a portable dilution sampling system and the effects of residence time on mass emission rates. *Aerosol Sci. Technol.* **2005**, *39,* 542−553.
(30) Simoneit, B. R. T.; Rogge, W. F.; Mazurek, M. A.; Standley, L. J.; Hildemann, L. M.; Cass, G. R. Lignin pyrolysis products, lignans, and resin acids as specific tracers of plant classes in emissions from biomass combustion. *Environ. Sci. Technol.* **1993**, *27*, 2533−2541.
(31) Rogge, W. F.; Hildemann, L. M.; Marurek, M. A.; Cass, G. R. Sources of fine organic aerosol. 1. charbroilers and meat cooking operations. *Environ. Sci. Technol.* **1991**, *25*, 1112−1125.
(32) Bilde, M.; Pandis, S. N. Evaporation rates and vapor pressures of individual aerosol species formed in the atmospheric oxidation of α- and β-pinene. *Environ. Sci. Technol.* **2001**, *35,* 3344−3349.
(33) Sheehan, P. E.; Bowman, F. M. Estimated effect of temperature on secondary organic aerosol concentrations. *Environ. Sci. Technol.* **2000**, *35,* 2129.
(34) Stanier, C. O.; Donahue, N. M.; Pandis, S. N. Atmospheric secondary organic aerosol yields: Model parameter estimation from smog chamber results. *Environ. Sci. Technol.* **2006**, submitted.
(35) Pathak, R. K.; Stanier, C. O.; Presto, A. A.; Donahue, N. M.; Pandis, S. N. Ozonolysis of α-pinene: Temperature dependence of secondary organic aerosol yields and their parameterization. *Environ. Sci. Technol.* **2006**, submitted.
(36) Kalberer, M.; Paulsen, D.; Sax, M.; Steinbacher, M.; Dommen, J.; Prevot, A. S. H.; Fisseha, R.; Weingartner, E.; Frankevic, V.; Zenobi, R.; Baltensperger, U. Identification of polymers as major components of atmospheric organic aerosols. *Science* **2004**, *303,* 1659.
(37) Ziemann, P. Evidence for low-volatility diacyl peroxides as a nucleating agent and major component of aerosol formed from reactions of O_3 with cyclohexene and homologous compounds. *J. Phys. Chem. A* **2002**, *106,* 4390.
(38) Kroll, J. H.; Ng, N. L.; Murphy, S. M.; Varutbangkul, V.; Flagan, R. C.; Seinfeld, J. H. Chamber studies of secondary organic aerosol growth by reactive uptake of simple carbonyl compounds. *J. Geophys. Res.* **2005**, *110*, D23207, doi: 10.1029/2005JD006004.
(39) Rudich, Y. Laboratory perspectives on the chemical transformations of organic matter in atmospheric particles. *Chem. Rev.* **2003**, *103,* 50975124.
(40) Molina, M. J.; Ivanov, A. V.; Trakhtenberg, S.; Molina, L. T. Atmospheric evolution of organic aerosol. *Geophys. Res. Lett.* **2004**, *31,* L22104 doi: 10.1029/2004GL020910.
(41) Donahue, N. M.; Hartz, K. E. H.; Chuong, B.; Presto, A. A.; Stanier, C. O.; Rosenhorn, T.; Robinson, A. L.; Pandis, S. N. Critical factors determining the variation in SOA yields from terpene ozonolysis: A combined experimental and computational study. *Faraday Discuss.* **2005**, *130,* 295−309.
(42) Robinson, A. L.; Donahue, N. M.; Rogge, W. F. Photochemical oxidation and changes in molecular composition of organic aerosol in the regional context. *J. Geophys. Res.* **2006**, *111*, D03302, doi: 10.1029/2005JD006265.
(43) Presto, A. A.; Donahue, N. M. Investigation of α-pinene + ozone secondary organic aerosol formation at low total aerosol mass. *Environ. Sci. Technol.* **2006**, in press.
(44) Claeys, M.; Graham, B.; Vas, G.; Wang, W.; Vermeylan, R.; Pashynska, V.; Cafmeyer, J.; Guyon, P.; Andreae, M.; Artaxo, P.; Maenhaut, W. Formation of secondary organic aerosols through photooxidation of isoprene. *Science* **2004**, *303,* 1173.
(45) Kroll, J. H.; Ng, N. L.; Murphy, S. M.; Flagan, R. C.; Seinfeld, J. H. Secondary organic aerosol formation from iosprene photooxidation. *Environ. Sci. Technol.* **2006**, in press.
(46) Atkinson, R. Gas-phase tropospheric chemistry of organic compounds. *J. Phys. Chem. Ref. Data* **1994**, *Monograph 2,* 216pp.
(47) Millet, D. B.; Donahue, N. M.; Pandis, S. N.; Polidori, A.; Stanier, C. O.; Turpin, B. J.; Goldstein, A. H. Partitioning VOCs and organic aerosols into primary and secondary sources: Results from the Pittsburgh Air Quality Study. *J. Geophys. Res.* **2005**, *110,* D07S07.

(48) de Gouw, J. A.; Middlebrook, A. M., Warneke, C.; Goldan, P. D.; Kuster, W. C.; Roberts, J. M.; Fehsenfeld, F. C.; Worsnop, D. R.; Canagaratna, M. R.; Pszenny, A. A. P.; Keene, W. C.; Marchewka, M.; Nertram, S. B.; Bates, T. S. Budget of organic carbon in a polluted atmosphere: Results from the New England Air Quality Study in 2002. *J. Geophys. Res.* **2005,** *110,* D16305.

(49) McFiggans, G.; Alfarra, M. R.; Allan, J.; Bower, K.; Coe, H.; Cubison, M.; Topping, D.; Williams, P.; Decesari, S.; Facchini, C.; Fuzzi, S. Simplification of the representation of the organic component of atmospheric particulates. *Faraday Discuss.* **2005**, *130,* 130/19.

(50) Zhang, Q.; Worsnop, D. R.; Canagaratna, M. R.; Jimenez, J.-L. Hydrocarbon-like and oxygenated organic aerosols in Pittsburgh: Insights into sources and processes of organic aerosols. *Atmos. Chem. Phys.* **2005**, *5,* 3289

Received for review November 14, 2005. Revised manuscript received January 16, 2006. Accepted February 10, 2006.

ES052297C